JOURNAL OF MATERIALS SCIENCE **39** (2004) 4553–4560

Laser *in-situ* synthesis of mixed carbide coating on steel

A. SINGH, N. B. DAHOTRE*
Center for Laser Application, Department of Materials Science and Engineering, University of Tennessee, Knoxville, Tennessee, USA
E-mail: ndahotre@utk.edu

A 2.5 KW Nd:YAG laser was employed to modify the surface of a AISI 1010 steel deposited with a precursor powder mixture of Fe, Ti, Cr and C. *In-situ* formation of TiC and chromium carbides [M_7C_3 (M = Fe, Cr) and Cr_7C_3] was observed as function of laser processing power at constant scan speed. Although TiC was present in all the samples, the chromium carbides were absent in samples processed at certain laser powers. Corresponding to this behavior, variation in mechanical properties of the coating was observed. The hardness and wear properties of the samples without chromium carbides was inferior in comparison to samples with both TiC and chromium carbides. © *2004 Kluwer Academic Publishers*

1. Introduction

The unending search for novel materials with superior tribological properties has lead to significant developments in the field of laser surface engineering (LSE). LSE is a technique for improving surface related properties (viz. hardness, wear and corrosion resistance) by modification of the surface layer of a bulk component using laser as the source of energy. The melt pool generated due to interaction of laser beam with the material undergoes rapid solidification, which provides a unique opportunity for non-equilibrium synthesis of materials. The refined volume of melt pool coupled with conduction mode of heat transfer enables synthesis of highly refined microstructures. Even metastable phases, which are not easily attainable by conventional processes, can be achieved by LSE. Such microstructures are known to have higher hardness and superior wear properties. The greatest advantage of this process is that the surface structure can be designed as per the requirements of the application by varying the processing parameters, which include beam power, beam size, scan speed and the composition of the precursor.

The importance of surface properties has increased tremendously in recent times with considerable amount of stress on improving it by forming a composite coating on the surface of a material rather than forming a relatively expensive bulk composite. Metal matrix composites have been known to have high hardness and exceptional wear resistance [1]. Carbide particles have often been incorporated in a Fe matrix to form a composite due to its inherent high hardness even at high temperatures. By careful selection of the type of carbides, it is possible to design a composite for severe abrasive conditions. TiC with exceptional hardness (Knoop Hardness 2800 kg/mm^2) [2] and thermal stability (decomposition temperature 3065°C) [2] has been frequently used as reinforcement in Fe based composites [3]. For the particles to be successfully incorporated, the melt should sufficiently wet the carbide particles. Ramquist [4] has shown that TiC particles are easily wetted by iron at high temperatures. Moreover, the wetting improves with temperature because of chemical interaction. It has also been shown that metals with an unfilled d band wet carbides more easily than metals with a filled d band [4]. Iron has an unfilled 3d orbital and hence wets TiC easily.

In the past TiC particle reinforced ferrous composites have been synthesized by a powder metallurgy route [5, 6]. TiC particles have been used as reinforcements on the surface of steel and Al by laser cladding [7, 8], electron beam [9] and plasma transferred arc [1]. In all these processes different amount of TiC powder was added. But, in recent years, emphasis has been given to the *in-situ* formation of TiC in an iron based matrix for several important reasons. The process is more economical and has an intrinsic advantage that the surface of the reinforcements is cleaner and hence the bond between the reinforcing particles and the matrix tends to be stronger. *In-situ* formation of TiC in cast iron [10, 11] and cast steel [12] has been reported in the past by various processes like cast sintering, solidification processing etc. Recently, Wu [13] developed a Ni alloy composite coating reinforced with *in situ* formed TiC on 5CrMnMo steel using laser cladding.

In addition to this, the Fe-Cr-C system has been used for hard facing of materials as Cr has a high tendency to form hard carbides, suitable for applications where high wear resistance is required [14]. Also, quaternary systems Fe-Cr-X-C (X = W, Mn) have been studied in

*Author to whom all correspondence should be addressed.

the past and the formation of M_7C_3 carbides has been shown with high degree of grain refinement [15].

All the above mentioned references have attempted to synthesize only one type of the coating composition where as on the contrary, the present work attempts to simultaneously synthesize a combination of carbide coatings (Ti and Cr based) in various amounts as function of laser processing parameters. The present study is aimed at employing the Fe-Ti-Cr-C quaternary system to engineer the surface of plain carbon steel for *in-situ* formation of both Ti and Cr based carbides using LSE (Laser Surface Engineering). In view of this, a direct comparison between these works and the current work deemed not justifiable.

During LSE, a part of the substrate along with the predeposited precursor layer is melted, mixed and solidified for a modified surface layer. The surface composite thus formed consists of *in-situ* formed carbides, which not only improve the hardness and wear resistance of the substrate, but also have the inherent advantage of being uncontaminated.

2. Experimental procedures

AISI 1010 steel (low carbon steel with a nominal 0.10 wt% C) was used as the substrate material in the present study, with the coating being an Fe- based alloy containing Ti, Cr and C. Rectangular plates (7.5 cm × 5 cm × 0.5 cm) of the substrate were sand blasted followed by washing with acetone and methanol to provide a clean and consistent surface. A mixture of commercially available Fe (99.9% pure), Ti (99.5% pure), C (99.5% pure) (all having average particle size $<45\ \mu$m) and Cr (99.8% pure, average particle size 10 micron or less) powders, supplied by CERAC, Milwaukee WI, were used as a precursor material. 20 wt% Ti, 20 wt% Cr, 5 wt% C and rest Fe powder were blended together and suspended in a water soluble organic binder to form a thick slurry. The slurry of precursor material was air spray deposited on the substrate for uniform green (unprocessed) thickness and then dried at 75°C for 30 min.

A 2.5 KW Hobart continuous wave Nd: YAG laser equipped with a fiber optic beam delivery system was employed for laser surface engineering. Fig. 1 depicts a schematic outline of the steps involved during laser processing of the as- received AISI 1010 steel sample. Parallel tracks with partial overlapping (∼15%) were laid with the laser beam focused 0.5 mm above the surface of the substrate. A range of different beam powers was used over a set of samples keeping the laser scan speed constant to 1500 mm/min. Argon was used as cover gas. The nozzle and working distance was kept constant at 20 mm to 132 mm respectively for all the processing powers. Table I lists the processing parameters used for the study.

TABLE I Processing parameters used for laser treatment

Sample no.	Power (W)	Scan velocity (mm/min)
A1	900	1500
B1	1300	1500
A2	1500	1500
B2	1900	1500
A3	2100	1500

The characterization of the coating was done by using optical microscopy, scanning electron microscopy (SEM), X-ray diffractometery (XRD), microhardness tester and dry sliding wear test. Samples were sectioned perpendicular to the laser processing direction and mounted in bakelite. The cross-section of the laser treated sample was polished using 400, 600, 800 and 1200 grit SiC pads (supplied by Buehler) and then alumina slurry on a microcloth. Microstructural characterization of the polished and etched samples was done on a Hitachi S3500 SEM. The samples were over etched so that the fine microstructure achieved during laser processing can be revealed and a sharp contrast between the carbide particles and the matrix can be obtained. X ray diffraction studies of the coating were conducted to identify and characterize the various phases present in the laser modified surface region. A Phillips Norelco X-ray diffractometer with Cu K_α radiation (1.54 Å), operated at 40 kV and 20 mA, was used for this. The specimen was scanned at a step size of 0.02 deg and for a count time of 1s with diffraction angles varying between 20 and 100 degrees.

Cross-section of samples polished in the way described earlier was subjected to microhardness test. Microhardness measurement was performed on a LECO

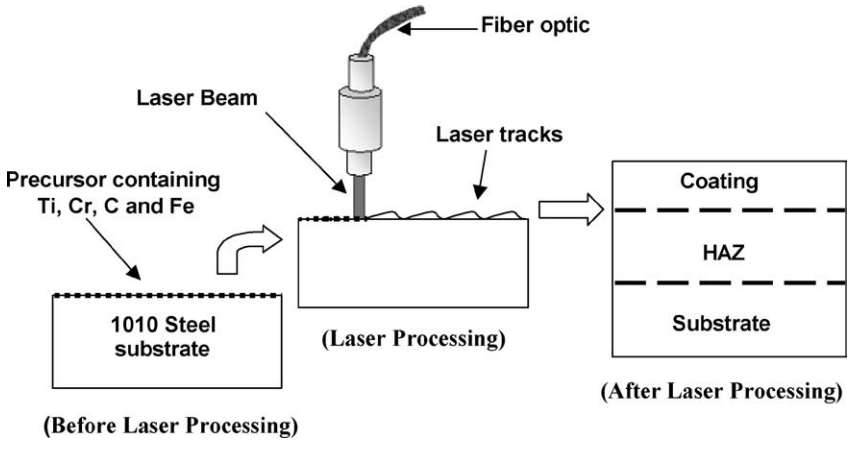

Figure 1 Schematic showing the steps in laser processing of the substrate.

microhardness tester LM 300AT with a Knoop indenter. A normal load of 100 g was applied for 15 s during the test. Indentations were made across the coating into the substrate at an interval of 50 μm. Dry sliding wear tests were performed on in-house built block-on-disk equipment. The tests were conducted on both substrate and coated samples. The weight loss during wear is an indication of the wear resistance of the sample. A normal load of 5.2 kgf was applied during the test. The wheel used to wear the samples was 4130 HT steel (65 Rc) and it was translated at 44 ms^{-1} linear speed. Weight of the samples was noted at every 2 min interval for a total period of 10 min to estimate the loss of material due to wear.

3. Results and discussion

The scanning electron micrograph of the cross section of the steel sample after laser surface treatment is illustrated in Fig. 2a. The sample was over etched with 5% nital to get a sharp contrast between carbide particles and matrix during SEM analysis. A uniform, adherent and crack free coating along with the heat-affected zone and the as-received substrate material is depicted in the figure. The substrate AISI 1010 steel has a nominal 0.10 wt% C and consists mainly of coarse grains of ferrite with few lamellae of pearlite within intergranular regions. During laser processing, the interaction of laser with substrate is only up to a limited depth due to the very high speed involved in the process and hence the substrate remains unaffected below a certain depth (approximately 350 μm) (Fig. 2b).

The heat affected zone (HAZ) is a transition region between the coating and the unaffected base material. In a higher magnification image (Fig. 2c), HAZ consisting of martensite plates having different orientations and the habit plane (the preferred crystal plane of austenite on which martensite crystal forms) is shown. This heat-affected zone has a distinctly sharp interface with the coating region (Fig. 2a). Within the coating region, there is a martensitic matrix with finely dispersed carbide particles (Fig. 2d). These carbides were formed *in-situ* during laser processing. The coating depth was found to be 200 $\pm$ 15 μm. The presence of martensite plates in both the HAZ and the coating was expected due to the very high cooling rates associated with laser processing of materials. X-ray diffraction analysis (XRD) (discussed later) further confirmed the presence of characteristic peaks of martensite and carbides in the coating. A large refinement of grains along with *in-situ* formation of carbides during processing is expected to lead to improvement in strength and hardness of the steel.

XRD analysis provided the presence and identification of various phases in surface and subsurface regions of laser processed samples. This included TiC, Fe-Cr, M_7C_3, Cr_7C_3, α' (martensite) and γ (austenite) (Fig. 3). Furthermore, based on the XRD analysis, a distinct pattern for the type of phase formation, as a function of laser power was noticed and accordingly it is divided into 2 groups. The first group of samples possessed the phases TiC, Fe-Cr, M_7C_3, Cr_7C_3, α', γ while the second group of samples possessed TiC, Fe-Cr, α'. The spectra of the two groups have been designated as Pattern 1 (Group 1) for samples A1 (900 W), A2 (1500 W) and A3 (2100 W) and Pattern 2 (Group 2) for samples B1 (1300 W) and B2 (1900 W) respectively in Fig. 3. A schematic outline of the variation in the reaction products as a result of the laser processing at different powers is presented in Fig. 4. Such a definite pattern in the evolution of phases was verified by processing and analyzing the samples twice under identical conditions.

The various phases present in the spectra, their crystal structures along with the space groups and lattice parameters are enlisted in Table II. Since Ti is very strong carbide former, as expected, all the samples show

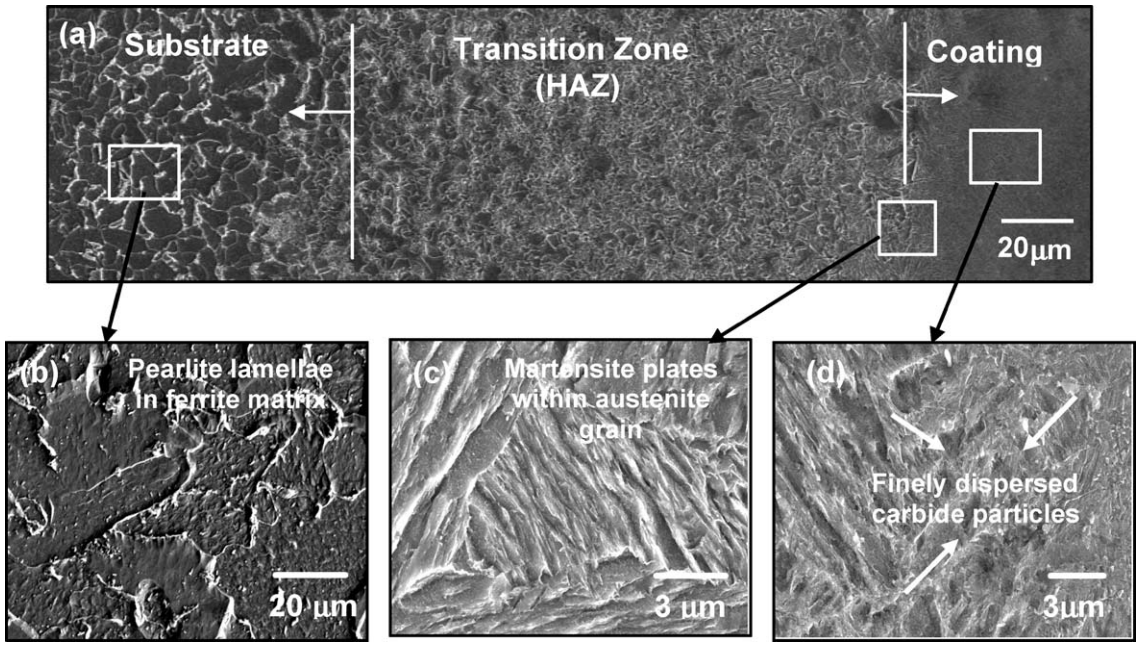

Figure 2 Scanning electron micrograph of sample processed at 1500 W. (a) Overview of the cross-section and high magnification images of (b) substrate, (c) transition zone and (d) coating region.

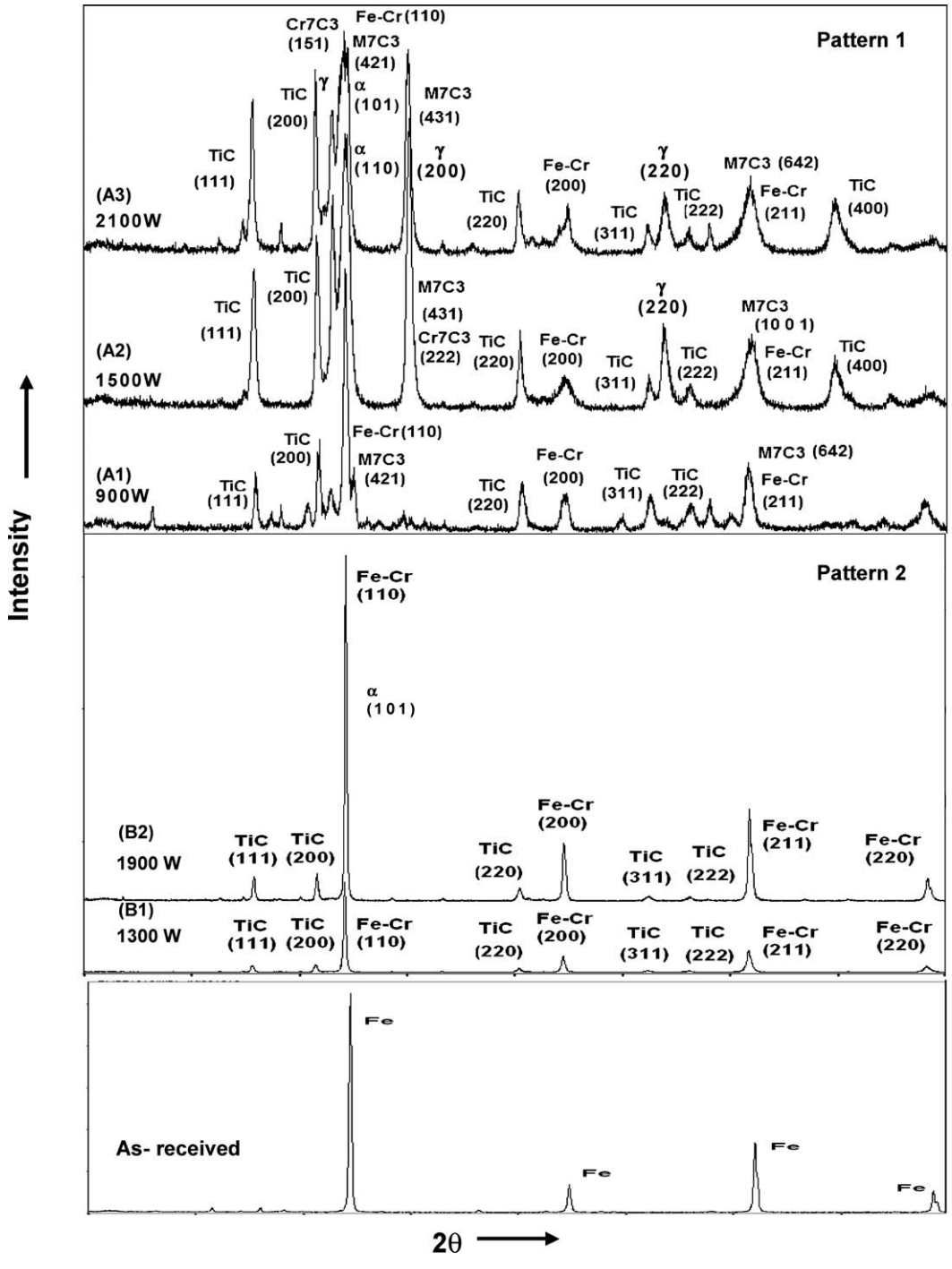

Figure 3 Overlay of X-ray Diffraction spectra of laser processed (900, 1300, 1500, 1900 and 2100 W) and as-received (unprocessed) samples.

prominent peaks of TiC thus confirming *in-situ* formation of TiC. In addition to this, the intensity of TiC peak increases with the beam power used for laser processing. Another phase, ferrite Fe-Cr (α), a substitutional solid solution of Cr in Fe is prominently present in all the samples. It is well known that Cr is a ferrite stabilizer [16] and helps in improving the strength and toughness of ferrite in steels. Also, according to Hume Rothery laws [17], the range of solubility in solid solution can be determined by (a) Chemical structure factor (b) Relative size factor (c) Chemical affinity factor (d) Relative valence factor. The crystal structure of both Cr and Fe is bcc as is the structure of Fe-Cr (as suggested by the space group of Fe-Cr mentioned in Table II). The relative size factor implies that if the difference in the atomic radii of the two elements involved is less than about 15%, the chances of formation of solid solution is high. The difference between the atomic radii of Fe and Cr is 0.4% as the atomic radii of Cr and Fe is 2.49 Å and 2.48 Å respectively. The chemical affinity of elements increases depending on how far they are separated in the periodic table; Fe and Cr are separated only by one element and hence they have low chemical affinity. The chance of forming solid solution increases with decrease in chemical affinity. The relative valence factor suggests that a metal with a lower valence tends to dissolve a metal with higher valence more than vice versa. Fe has a lower valence than Cr and hence tends to dissolve it more. Thus, the formation of Fe-Cr phase as a result of the laser processing can be comprehended.

TABLE II List of various phases identified during XRD

Phase	Crystal structure	Space group	Lattice parameter	Samples in which present
TiC	Cubic	Fm3m	$a = 4.33$ Å	A1, A2, A3, B1, B2
Fe-Cr	Cubic	Im3m	$a = 2.88$ Å	A1, A2, A3, B1, B2
M_7C_3	Hexagonal close packed	P31c	$a = 13.98$ Å, $c = 4.52$ Å	A1, A2, A3
Martensite (α')	Tetragonal	I4/mmm	$a = 2.86$ Å, $c = 2.96$ Å	B1, B2, A2, A3
Austenite (γ)	Cubic	Fm3m	$a = 3.60$ Å	A2, A3
Cr_7C_3	Orthorhombic	PmCm	$a = 7.01$, $b = 12.53$, $c = 4.53$	A1, A2, A3

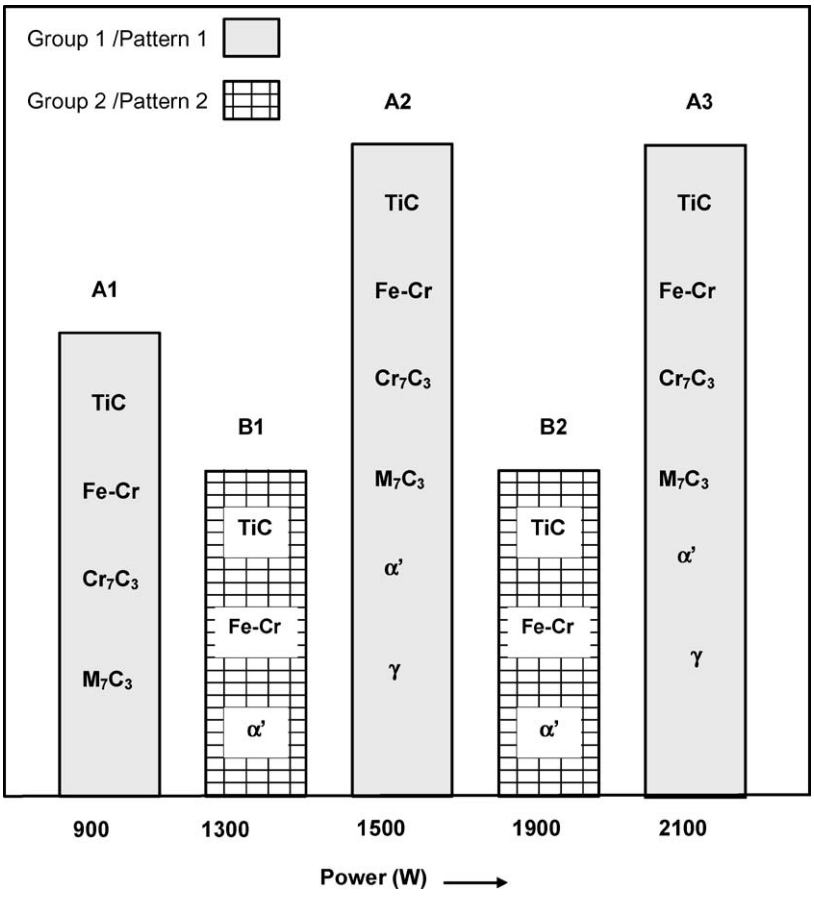

Figure 4 Schematic of reaction products as a function of laser processing power.

The spectra of samples A1, A2 and A3 indicated the presence of a phase M_7C_3 (M = Cr, Fe), which is a complex carbide of a hexagonal close packed structure and has a lattice parameters of $c = 4.52$ Å and $a = 13.98$ Å. The formation of such complex chromium carbide can be attributed to the high concentration of Cr in the precursor coating and to the rapid cooling rate associated with laser processing. Also, in the present Fe-Ti-C system, TiC formation occurred with Ti depletion in the system that could lead to the tendency of Fe to form cementite. But, since a high percentage of Cr (20 wt%) was present in the precursor alloy, formation of Cr_7C_3 and M_7C_3 type carbides took place rather than Fe_3C as Cr has a higher tendency to form carbides than iron. The various reaction equations accompanied by their respective free energy changes for the formation of carbides from respective elemental state has been listed in Table III [18]. The free energy values help in predicting the formation of carbides relative to each other.

As indicated in Fig. 5 for the free energy of formation of the carbides with respect to temperature, Ti and Cr have stronger carbide forming tendency than Fe. (The free energy values are much lower for both TiC and Cr_7C_3 than Fe_3C). Interestingly, the free energy value for Cr_7C_3 is much lower than TiC for most of the temperature range (298–2000 K). However, on the contrary, the experimental observations indicated TiC

TABLE III Free energy of reaction as function of temperature

Reaction	Free energy (J/ mole)	Temperature range (°K)
(1) Ti + C = TiC	−183172 + 10.09 T	298–1155
	−186731 + 13.2 T	1155–2000
(2) 7Cr + 3C = Cr_7C_3	−174401 − 25.9 T	298–2171
	−360902 + 60.08 T	2171–2938
(3) 3Fe + C = Fe_3C	25958 − 23.27 T	298–463
	26711 − 24.78 T	463–1115
	1036 − 10.17 T	1115–1808

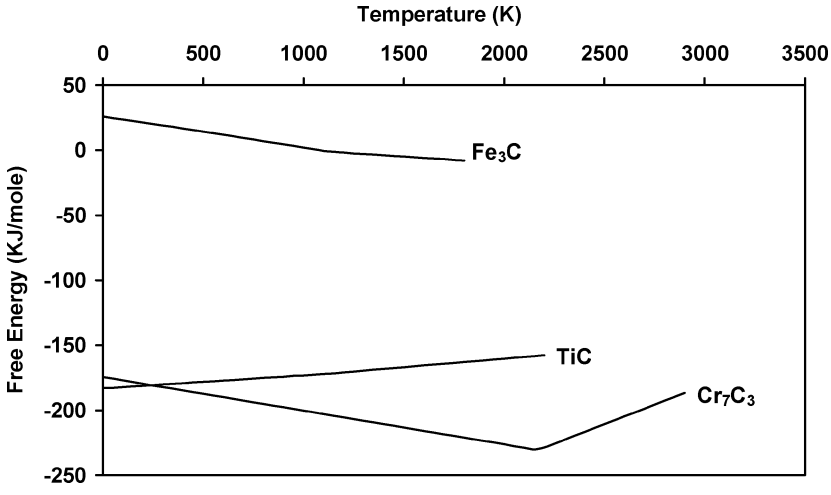

Figure 5 Variation of free energy of carbides with temperature.

as prominently present in all the samples (Table II) and absence of Cr_7C_3 in samples B1 and B2. In view of this, it can be postulated that as the tabulated free energy values are for pure elements, the presence of both Ti and Cr would affect the activity of each of them. This might influence the type of carbides formed. This corroborates the fact that LSE is a non equilibrium process and formation of metastable phases can take place as a result of the rapid speed of the process.

While the high cooling rates in the laser processing of materials formed metastable phases like martensite (A2, A3, B1 and B2 in Fig. 3), the presence of retained austenite peaks (in samples A2 and A3) can be attributed to the fact that 5 wt% C was added in the precursor and C being a very strong austenite stabilizer, reduces the M_s (Martensite start) temperature considerably. The absence of both retained austenite and martensite in the sample A1 (Figs 3 and 4) is probably due to lower power of processing (900 W) and hence lower temperature of the substrate leading to slower cooling rate.

The essential difference between the Group 1 (A1, A2 and A3) and Group 2 (B1 and B2) is the presence of Cr- carbides in the former and its absence in the latter, although TiC is present in all samples. At the powers used for processing samples in group 2, the entire chromium appeared to have gone into a solid solution with Fe to form Fe-Cr thereby preventing the formation of Cr-carbides. An approximate estimate of this solid solution present in respective samples is ascertained by calculating the ratio of integrated intensity of Fe-Cr (α) peaks to integrated intensity of the entire spectrum of the sample. (Table IV) The quantitative analysis is based on the fact that the intensity of the diffraction pattern of any specific phase in a mixture of phases is dependent on the concentration of that phase in the mixture [19]. This ratio is higher in samples B1 and B2 (>0.85) than in samples A1, A2 and A3 (<0.40).

To correlate the effect of type and variation in the phase evolution with the properties, mechanical characterization was conducted for microhardness and wear properties. In general, microhardness values indicate a tremendous improvement in hardness of the steel substrate due to the laser surface modification. Nearly a 5-fold improvement in the hardness of the surface of the as-received sample processed at different laser powers is observed (Fig. 6). The hardness profile of all the samples indicates that the hardness is higher in the coating region and gradually decreases through the heat affected zone (transition zone) into the substrate. The hardness values show some variation through heat-affected zone. The higher hardness of the coating can be attributed to the *in-situ* formation of various carbides in the coating region. The Knoop hardness values in the coating for samples in group 1 (A1 and A2) are higher than the samples in group 2 (B1 and B2). (Fig. 6). The potential reason for this behavior is the absence of Cr-carbides in Group 2 and its presence in Group 1, with TiC being present in both (Figs 3 and 4).

During the dry sliding wear studies, the cumulative weight loss of the laser-processed samples was found to be negligible in comparison to the AISI 1010 steel substrate (Fig. 7). This clearly indicated a vast improvement in the wear resistance of the steel substrate due to the presence of carbides in the coating region. The weight loss of the coated samples is nearly 4 times less than that for the as-received sample. Also, as the figure shows, the cumulative weight loss of the as-received sample becomes almost constant after some time due to strain hardening effects.

Among the samples processed at different powers, it was seen that the sample processed at 1900 W had the least wear resistance. This is the same sample which has lower hardness and has absence of chromium carbides (Figs 3 and 4). On the contrary, the other sample from the same group, which had no chromium carbides, B1

TABLE IV Ratio representing an approximate estimate of the relative amount of Fe-Cr present in samples processed at various powers

Processing power (sample)	Estimated amount of Fe-Cr*
900 W (A1)	0.388
1300 W (B1)	0.859
1500 W (A2)	0.920
1900 W (B2)	0.871
2100 W (B3)	0.239

*Ratio of integrated intensity of Fe-Cr to the integrated intensity of entire spectrum.

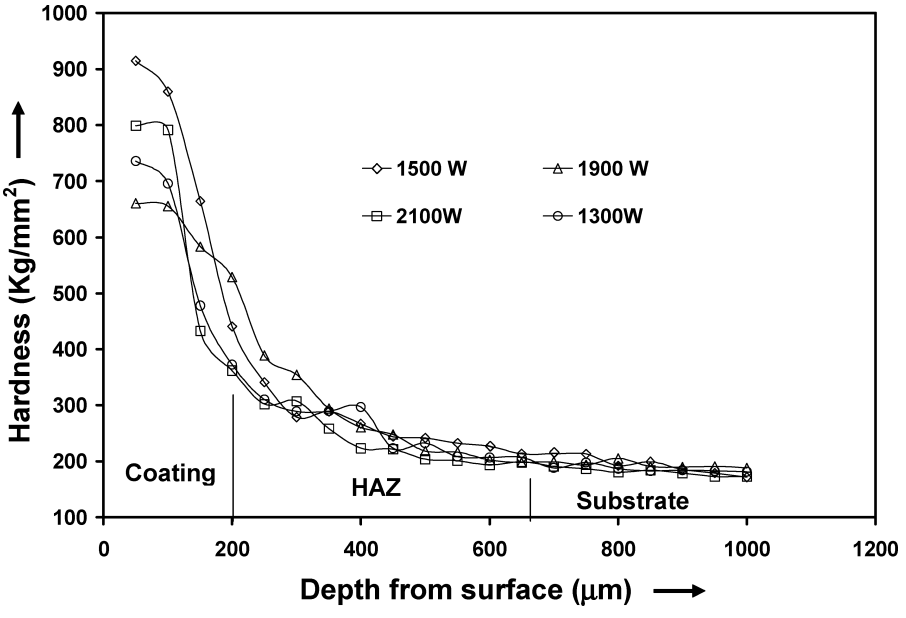

Figure 6 Hardness profiles for laser processed samples.

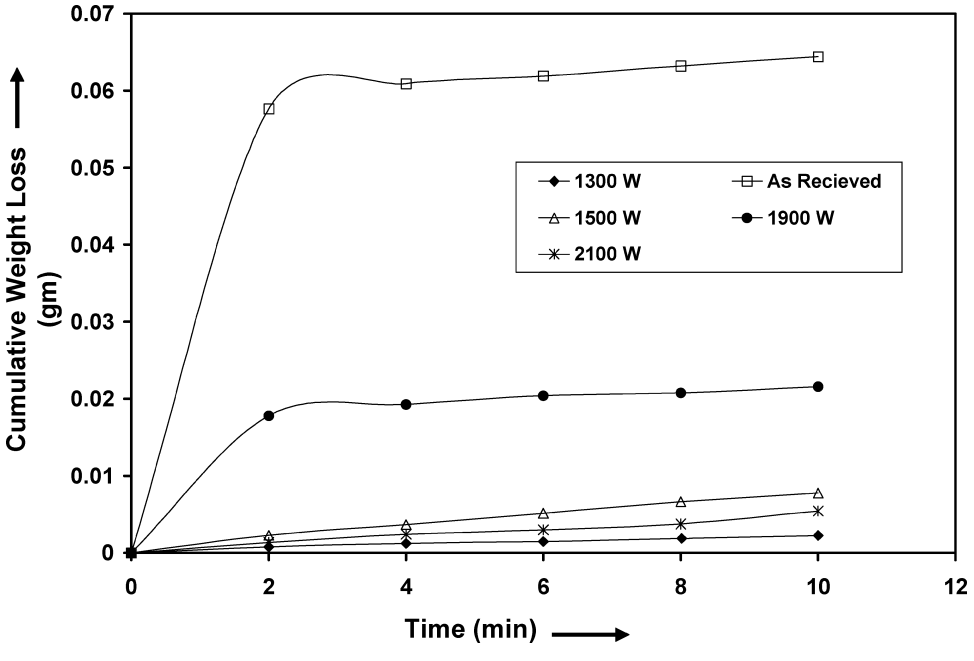

Figure 7 Cumulative weight loss as function of time during dry sliding wear.

(1300 W) indicated very low cumulative weight loss. Such contrast in wear behavior from the same group of samples could be attributed to the physical nature of the laser processed surface, which was evaluated by surface roughness measurement. The measurements show that for the sample processed at 1300 W (B1), R_a (arithmetic mean roughness) = 9.198 μm, R_z (average maximum height) = 48.2 μm whereas for the sample processed at 1900 W (B2) has $R_a = 1.476$ μm, $R_z = 9.34$ μm. This indicates that the former is relatively rougher in comparison to the latter, thus the surface area of the sample in contact with the wheel during sliding wear was less in the case of B1 and hence the low weight loss.

Thus laser surface engineering is a versatile technique to manufacture the surface of a component to tailor its mechanical properties via *in-situ* phase formation.

4. Conclusions

In-situ formation of various types and combinations of carbides on a plain carbon steel (AISI 1010) was achieved with laser based processing technique. TiC was prominently present in the surface layer of all the samples and chromium carbides were found to be absent in the samples processed at 1300 W and 1900 W. This variation in phase evolution had strong influence on mechanical properties. The hardness and wear properties of the samples without chromium carbides were inferior to the samples with both TiC and chromium carbides. A substitutional solid solution of chromium in iron (Fe-Cr) was found in all the samples and the relative estimated amount of the phase was higher for the samples without chromium carbides. Metastable phase (characteristic of non-equilibrium synthesis) like martensite was present in the coating and transition

zone. Thus, the formation of carbide composite surface layer provided a 5-fold improvement in the hardness (maximum hardness in coating 914 HK) of the surface (180 HK) for the as-received steel.

Acknowledgments

The authors would like to express their sincere thanks to Mr. Fred Schwartz for assistance with the experimental work. The continuous help and support of Subhadarshi Nayak and Abhijeet Khangar (graduate students) is gratefully acknowledged.

References

1. L. BOURITHIS, ATH. MILONAS and G.D. PAPADIMITRIOU, *Surface and Coatings Tech.* **165** (2003) 286.
2. B. BHUSHAN and B. K. GUPTA, in "Handbook of Tribology: Materials, Coatings and Surface Treatments" (McGraw-Hill, NY, 1991) p. 4.53.
3. YISAN WANG, XINYUAN ZHANG, FENGCHUN LI and GUANGTING ZENG, *Mater. and Design* **20** (1999) 233.
4. L. RAMQVIST, *Int. J. Powder Metall.* **4** (1965) 1.
5. M. M. OLIVEIRA and J. D. BOLTON, *J. Mater. Process.* **92/93** (1999) 15.
6. E. PAGOUNIS, M. TALVITIE and V. K. LINDROOS, *Metall. Mater. Trans.* **27A** (1996) 4171.
7. T. C LEI, J. H. OUYANG, Y. T. PEI and Y. ZHOU, *Mater. Sci. Tech.* **11** (1995) 520.
8. L. R. KATIPELLI, A. AGARWAL and N. B. DAHOTRE, *Appl. Surf. Sci.* **153** (2000) 65.
9. S.-J. KWON, S.-H. CHOO and S. LEE, *Scripta Materialia* **40**(2) (1999) 235.
10. C. RAGUNATH, M. S. BHAT and P. K ROHATGI, *Scripta Metallurgica et Materialia* **32**(4) (1995) 577.
11. Y. WANG, X. ZHANG, G. ZEN and F. LI, *Composites* A **32** (2001) 281.
12. V. K. RAI, R. SRIVASTAVA, S. K. NATH and S. RAY, *Wear* **231** (1999) 265.
13. X. WU, *Surface and Coatings Technology* **115** (1999) 111.
14. L. E SVENSSON, B. GRETOFT, B.ULANDER and H. K. D. H. BHADESHIA, *Surface Eng. Con.* **2** (1985) 75.
15. K. NAGARATHNAM and K. KOMVOPOULOS, *Metall. Trans.* A **24** (1993) 1621.
16. S. H. AVNER, in "Introduction to Physical Metallurgy" (McGraw-Hill, Singapore, 1974) p. 350.
17. *Idem.*, in "Introduction to Physical Metallurgy" (McGraw-Hill, Singapore, 1974) p. 152.
18. G. V. SAMSONOV and I. M. VINITSKII, in "Handbook of Refractory Compounds" (IFI/Plenum Data Company, New York, 1980) p. 140.
19. B. D. CULLITY, in "Elements of X-Ray Diffraction" (Addison-Wesley, Philippines, 1978) p. 407.

Received 5 June
and accepted 1 April 2004